Functional characterization of pulmonary neuroendocrine cells in lung development, injury, and tumorigenesis

Hai Song, Erica Yao, Chuwen Lin, Rhodora Gacayan, Miao-Hsueh Chen, and Pao-Tien Chuang[1]

Cardiovascular Research Institute, University of California, San Francisco, CA 94158

Edited* by Matthew P. Scott, Howard Hughes Medical Institute, Stanford University, Stanford, CA, and approved September 14, 2012 (received for review April 30, 2012)

Pulmonary neuroendocrine cells (PNECs) are proposed to be the first specialized cell type to appear in the lung, but their ontogeny remains obscure. Although studies of PNECs have suggested their involvement in a number of lung functions, neither their in vivo significance nor the molecular mechanisms underlying them have been elucidated. Importantly, PNECs have long been speculated to constitute the cells of origin of human small-cell lung cancer (SCLC) and recent mouse models support this hypothesis. However, a genetic system that permits tracing the early events of PNEC transformation has not been available. To address these key issues, we developed a genetic tool in mice by introducing a fusion protein of Cre recombinase and estrogen receptor (CreER) into the *calcitonin gene-related peptide* (*CGRP*) locus that encodes a major peptide in PNECs. The $CGRP^{CreER}$ mouse line has enabled us to manipulate gene activity in PNECs. Lineage tracing using this tool revealed the plasticity of PNECs. PNECs can be colabeled with alveolar cells during lung development, and following lung injury, PNECs can contribute to Clara cells and ciliated cells. Contrary to the current model, we observed that elimination of PNECs has no apparent consequence on Clara cell recovery. We also created mouse models of SCLC in which $CGRP^{CreER}$ was used to ablate multiple tumor suppressors in PNECs that were simultaneously labeled for following their fate. Our findings suggest that SCLC can originate from differentiated PNECs. Together, these studies provide unique insight into PNEC lineage and function and establish the foundation of investigating how PNECs contribute to lung homeostasis, injury/repair, and tumorigenesis.

progenitor | naphthalene | cell of origin | tumor suppressor gene

One of the major unresolved issues in the lung field is how undifferentiated epithelial cells generate specialized cell types in the postnatal lung (1–3). Another pressing challenge is to uncover the cell types and molecular mechanisms that underlie the enormous regenerative capacity of the lung during injury (4). The lung produces more than 40 cell types to fulfill the important roles of mucociliary clearance, gas exchange, and metabolic and endocrine function. The major cell types in lung epithelium include basal cells, ciliated cells, Clara cells, neuroendocrine cells, and type I and type II pneumocytes (Fig. S1 *A–F*). Pulmonary neuroendocrine cells (PNECs) are proposed to be the first specialized cell type to appear within the epithelium, implying that progressive cell-type specification in the lung starts with progenitors of neuroendocrine nature (5). However, the ontogeny of PNECs and their relationships to other lung cell types during normal homeostasis and lung injury remain unclear. Unlike some other cell types in the mammalian lung, PNECs are found in most species examined, including amphibians, reptiles, birds, mammals, and even in gill filaments of fish, suggesting an evolutionarily conserved function of PNECs in lung physiology across phyla.

Single PNECs are scattered in the respiratory epithelium, whereas clustered PNECs [called neuroepithelial bodies (NEBs)] are usually found in the intrapulmonary airways, often at airway bifurcations or bronchioalveolar duct junctions. PNECs are innervated at the basal part and have microvilli that protrude into the airway lumen at their apical surface. NEBs contain secretory granules and dense-core vesicles, which store various amines and peptides, including gastrin-releasing peptide (GRP), serotonin (5-HT), calcitonin gene-related peptide (CGRP), calcitonin, substance P, somatostatin, chromogranin A, and synaptophysin (SYP). These contents are released by physiological stimuli, such as hypoxia, and many of them have potent physiological effects. The diverse and often opposite effects of secreted amines and peptides from NEBs reveal the complex nature of PNEC function that remains to be elucidated. Decades of studies on PNECs culminate in the current view that PNECs function in airway oxygen sensing, regulate pulmonary blood flow, control bronchial tonus, modulate immune responses, and maintain a stem cell niche (5, 6). No other cell type in the lung exhibits such a diverse array of activities. However, many of these conclusions are derived from experiments using ex vivo tissue/organ culture or cell-based assays. Rigorous tests in a genetic model organism (e.g., mouse) to validate and pinpoint the major physiological functions of PNECs and uncover the molecular mechanisms have not been performed. The evolutionary conservation of PNECs implies that conclusions reached in mice can be extrapolated to other mammals, including humans.

NEBs are found in close association with secretory nonciliated Clara cells. Following naphthalene-induced lung injury (7, 8), which kills most Clara cells, the only surviving Clara cells (termed variant Clara cells in some literature) are located near NEBs and at the bronchioalveolar duct junction. These survivors are capable of restoring the damaged lung epithelium. These observations led to the hypothesis that PNECs maintain a stem cell niche essential for Clara cell regeneration during lung injury (9, 10). Whether such a niche actually exists or has functional importance has never been critically evaluated.

PNECs have also been implicated in a number of lung diseases. Perhaps the most important clinical connection comes from the observation that characteristic markers of PNECs are frequently expressed in human small-cell lung cancer (SCLC), a highly aggressive form of lung cancer related to cigarette smoking (11). This finding led to the speculation that PNECs could be the cells of origin for SCLC, an idea that has been supported by mouse studies (12–15). Despite this insight, the ability to reliably trace the early events that underlie changes in PNEC behavior and their progression toward tumor development in a defined genetic setting has not been achieved. As a result, a definitive answer to whether SCLC is derived from progenitors or differentiated cells is not available. Filling in the major gaps in our molecular understanding of PNEC transformation requires the development

Author contributions: H.S., E.Y., and P.-T.C. designed research; H.S., E.Y., C.L., R.G., M.-H.C., and P.-T.C. performed research; H.S., E.Y., and P.-T.C. analyzed data; and H.S., E.Y., and P.-T.C. wrote the paper.

The authors declare no conflict of interest.

*This Direct Submission article had a prearranged editor.

[1]To whom correspondence should be addressed. E-mail: pao-tien.chuang@ucsf.edu.

This article contains supporting information online at www.pnas.org/lookup/suppl/doi:10.1073/pnas.1207238109/-/DCSupplemental.

of additional mouse models of SCLC that recapitulate critical aspects of human tumors.

To regulate gene activity specifically in PNECs, we introduced CreER into the endogenous mouse *CGRP* locus by gene targeting (Fig. S2*A*) because CGRP is the major peptide produced in PNECs. The resulting mouse line is designated $CGRP^{CreER}$. *CreER* encodes a fusion protein of Cre recombinase and estrogen receptor (ER), and CreER is active only when tamoxifen (TM) is present. Thus, TM administration to $CGRP^{CreER}$ mice provides an efficient way to control Cre activity in a temporally and spatially specific manner.

Results

Inducible Expression of CreER from the Mouse *CGRP* Locus Confers Spatial and Temporal Control of Gene Expression in Pulmonary Neuroendocrine Cells. To test the efficiency and specificity of CreER expression in $CGRP^{CreER}$ mice, we bred $CGRP^{CreER}$ mice with $ROSA26^{mTmG}$ reporter mice to generate mice carrying the genotype of $CGRP^{CreER/+}$;$ROSA26^{mTmG/+}$. Cre activation upon TM administration resulted in eGFP expression from the $ROSA26^{mTmG}$ allele. PNECs were identified using multiple markers, including anti-Ascl1 (Mash1), anti-CGRP, anti-SYP, anti-chromogranin A, and anti-PGP9.5. We detected GFP expression in 50–90% of $CGRP^{+}$ cells, and in some NEBs the efficiency reached almost 100% (Fig. S2 *B–G*). The specificity of CreER expression in PNECs was demonstrated by the observation that no eGFP expression was detected without TM (Fig. 1*F* and Fig. S2 *H–J*) or in $CGRP^{-}$ cells in $CGRP^{CreER/+}$;$ROSA26^{mTmG/+}$ lungs (Fig. S2 *B–G*). *R26R* reporter mice yielded similar results. These findings indicate that CreER expression from $CGRP^{CreER}$ mice is specific and sufficient to permit manipulating gene activity in PNECs.

Pulmonary Neuroendocrine Cells Are Colabeled with Alveolar Cells During Lung Development. Pulmonary neuroendocrine cells have been proposed to originate from the lung epithelium (instead of the neural crest). To test this, we took advantage of *Shh-Cre*, *Nkx2.1-Cre*, and *Sox9-Cre* mouse lines in which Cre is expressed broadly in the lung epithelium but not in the neural crest. We generated *Shh-Cre/+;R26R/+* mice in which constitutive epithelial Cre expression from the endogenous *Shh* locus would result in *LacZ* expression from the *R26R* reporter. Shh-Cre–mediated recombination can be detected in the lung epithelium as early as 9.5 days postcoitum (dpc). We found that PNECs together with other epithelial cell types yielded positive staining for β-gal (Fig. 1*A*), suggesting that epithelial cells give rise to PNECs. Similar results were obtained using *Nkx2.1-Cre/+;* $ROSA26^{mTmG/+}$ (Fig. 1*B*) or *Sox9-Cre/+;*$ROSA26^{mTmG/+}$ (Fig. 1*C*) mice. Our findings are consistent with the previous report that $Id2^{+}$ tip epithelial cells labeled at the pseudoglandular stage of mouse development contribute to all lineages, including neuroendocrine cells (16).

Our $CGRP^{CreER}$ mice provide a tool to follow the fate of $CGRP^{+}$ cells during lung development. We injected a single dose of TM into pregnant $CGRP^{CreER/+}$;$ROSA26^{mTmG/+}$ mice at different gestational ages and collected the lungs of progeny at postnatal day 30 or 60. This allowed us to label cells that express CreER by eGFP expression at a particular stage of lung development and follow the cell types they eventually generate. The identity of lung cells labeled by eGFP was determined by immunostaining using markers specific for distinct lung cell types (Fig. 1 *G* and *H* and Fig. S1 *A–F*). When the embryos were exposed to TM between 12.5 and 14.5 dpc, PNECs were labeled (Fig. 1*G*). Surprisingly, a small fraction of alveolar type I (stained with anti-T1α) and type II (stained with anti-SP-C) pneumocytes were also labeled (Fig. 1 *H* and *I*). Clusters of lineage-labeled type I cells are located within the same alveolus (arrows in Fig. 1*I*), suggesting that the cluster is derived from a common progenitor. By contrast, secretory Clara cells [stained with anti-Clara cell 10-kDa protein (CC10)] or ciliated cells (stained with anti-acetylated tubulin) were never labeled. These

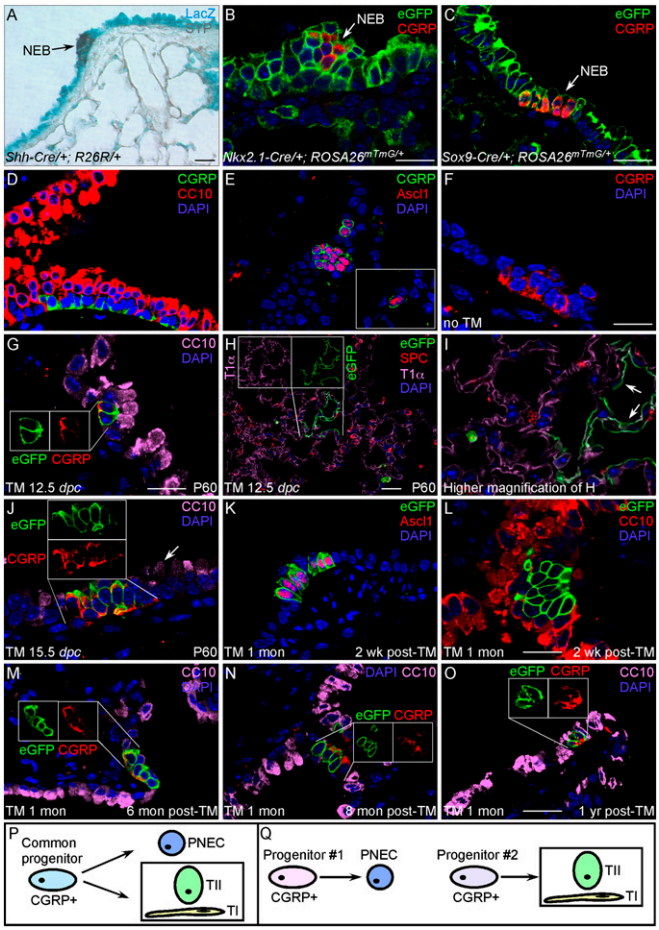

Fig. 1. Lineage tracing of PNECs in embryonic and postnatal lungs. (*A*) β-gal (LacZ) staining of lung sections from *Shh-Cre/+;R26R/+* adult mice. (*B* and *C*) Immunostaining of lung sections from *Nkx2.1-Cre/+;*$ROSA26^{mTmG/+}$ or *Sox9-Cre/+;*$ROSA26^{mTmG/+}$ adult mice. Extensive (nearly ubiquitous) labeling of epithelial cells by β-gal (blue) or eGFP (green) was observed. Labeled epithelial cells include clustered PNECs (NEBs; arrows), which were identified by anti-SYP (brown), anti-CGRP (red), or additional antibodies. (*D*) Immunostaining of lung sections from adult wild-type (WT) mice. PNECs ($CGRP^{+}$) are found in clusters and in close association with Clara cells ($CC10^{+}$). (*E*) Immunostaining of lung sections from adult WT mice. CGRP immunoreactivity coincides with that of Ascl1 (Mash1). (*Inset*) Solitary PNEC. (*F*) Immunostaining of lung sections from adult $CGRP^{CreER/+}$;$ROSA26^{mTmG/+}$ mice without TM injection. No eGFP-labeled cells were detected. (*G–I*) Immunostaining of lung sections from adult $CGRP^{CreER/+}$;$ROSA26^{mTmG/+}$ mice [postnatal day 60 (P60)] exposed to tamoxifen at 12.5 dpc. Activation of CreER by tamoxifen during embryogenesis led to eGFP labeling of PNECs (*G*) as well as alveolar cells, including type I ($T1\alpha^{+}$) and type II ($SP\text{-}C^{+}$) pneumocytes (*H* and *I*). (*H Inset*) Individual images of eGFP and CGRP immunostaining of the same cells. Arrows in *I* point to labeled type I cells. No Clara cells or other cell types were labeled by eGFP. (*J*) Immunostaining of lung sections from adult $CGRP^{CreER/+}$;$ROSA26^{mTmG/+}$ mice (P60) exposed to tamoxifen at 15.5 dpc. Only PNECs were labeled. Arrow points to unlabeled Clara cells. (*Inset*) Separate images of eGFP and CGRP immunostaining of the same cells. (*K–O*) Immunostaining of lung sections from adult $CGRP^{CreER/+}$;$ROSA26^{mTmG/+}$ mice injected with tamoxifen at 1 mo of age and analyzed at different time points post-TM injection. (*M–O Insets*) Individual images of eGFP and CGRP immunostaining of the same cells. (*P* and *Q*) A model of PNEC specification during lung homeostasis. (Scale bars: 25 μm for panels in each row.)

results suggest that PNECs may share a common origin with alveolar but not conducting cell types during early lung development. Alternatively, during development, $CGRP^{CreER}$ may label separate progenitor populations that give rise to PNECs and alveolar cells, respectively. Interestingly, when embryos were exposed to TM at

11.5 dpc, only a small number of type I and type II cells were lineage labeled, and no PNECs were labeled. If TM injection is performed at or after 15.5 dpc, only PNECs were labeled (Fig. 1*J*), suggesting that by ~15.5 dpc the PNEC lineage has segregated from other lineages. In our lineage-tracing studies (Table S1), no other lung epithelial cells or lung mesenchymal cells, such as fibroblasts or blood vessels, were labeled. Interestingly, a small number of muscle cells in the pulmonary veins that likely originate from cardiomyocytes (17) were labeled when TM was injected before 15.5 dpc (Fig. S3). $CGRP^{CreER}$ activity can also be detected in several mouse tissues other than the lung, consistent with the presence of a diffuse neuroendocrine system (Fig. S4).

We then asked whether the committed PNEC fate is stable during normal homeostasis in adult lungs. We injected $CGRP^{CreER/+}$;$ROSA26^{mTmG/+}$ mice with TM at 1–2 mo of age and analyzed cell types labeled by eGFP at 0, 2, 4, 6, 8, and 12 mo after injection (Fig. 1 *K–O*). In mice studied even at 1 y after TM injection, only PNECs remained labeled by eGFP (Fig. 1*O*), though the percentage of lineage-labeled PNECs within NEBs was slightly decreased, consistent with reduced PNEC number with age. No other cell types were labeled, which suggests that the fate of PNECs is steady in adult lungs during homeostasis (Table S2).

Pulmonary Neuroendocrine Cells Contribute to Clara Cells and Ciliated Cells During Lung Injury. Although the PNEC fate is stable in adult lungs during homeostasis, we wondered whether PNECs in the adult lung could serve as progenitors for other cell types during tissue injury. To test this, we used the well-established naphthalene-induced lung injury model to ablate Clara cells. We injected $CGRP^{CreER/+}$;$ROSA26^{mTmG/+}$ mice at 1–2 mo of age with TM to label PNECs, and this was followed by naphthalene injection. Exposure to naphthalene led to extensive death of Clara cells, followed by proliferation of the surviving Clara cells and subsequent restoration of lung epithelium by 1 mo (Fig. 2 *A–D*). The surviving Clara cells do not express a cytochrome P450 enzyme that metabolizes naphthalene to toxic epoxide.

In contrast with a very low rate of PNEC proliferation during homeostasis, the number of PNECs labeled by CGRP and Ki67 significantly increased after naphthalene injection (Fig. 2 *E–H*), indicating increased PNEC proliferation after lung damage. Interestingly, we also detected eGFP-labeled Clara cells and ciliated cells (Fig. 2 *I–L*), which suggests that unlike in development and homeostasis, following lung injury PNECs possess the capability of producing Clara cells and ciliated cells. We speculate that the labeled ciliated cells were derived from labeled Clara cells (produced from PNECs) because lineage tracing of Clara cells has revealed their potential to generate ciliated cells (18). No other cell types, including type I and type II pneumocytes, were labeled by eGFP in $CGRP^{CreER/+}$;$ROSA26^{mTmG/+}$ mice that received tamoxifen and naphthalene. These results argue a lineage relationship between PNECs and Clara cells during lung injury. Interestingly, lineage tracing of CC10-expressing cells (including variant Clara cells) actually shows no contributions of these cells to PNECs (18).

Pulmonary Neuroendocrine Cells Have Very Limited Potential to Regenerate After Ablation. Because lung epithelium can be replenished after lung injury, we investigated whether PNECs can be regenerated after ablation. We took advantage of efficient cell killing by diphtheria toxin (DTA) to genetically eliminate PNECs in mice, and performed crosses to obtain $CGRP^{CreER/+}$;$ROSA26^{DTA/+}$ mice. Induction of Cre expression in PNECs by TM injection should result in DTA expression from the $ROSA26^{DTA/+}$ allele by removing floxed sequences that block DTA expression. We tested the efficiency of cell killing by TM injection to adult $CGRP^{CreER/+}$;$ROSA26^{DTA/+}$ mice and collected lungs a few days after the last injection. Virtually no PNECs were detected when a battery of PNEC markers was used, indicating nearly complete eradication of PNECs (Fig. S5). By contrast, other lung cell types, such as Clara cells, ciliated cells, and type I and

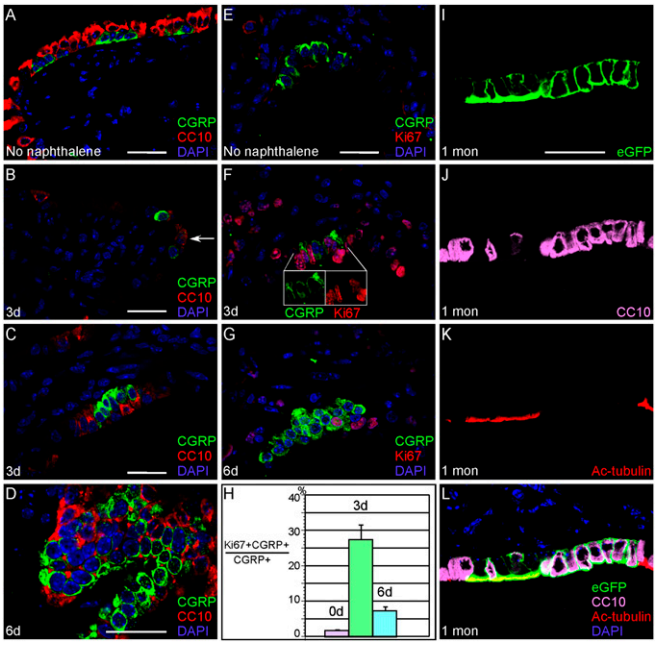

Fig. 2. CGRP$^+$ cells can give rise to Clara cells and ciliated cells during Clara cell regeneration induced by naphthalene administration. (*A–G*) Immunostaining of lung sections from adult $CGRP^{CreER/+}$;$ROSA26^{mTmG/+}$ mice. CreER in PNECs (CGRP$^+$) of adult lungs was activated by TM injection and followed by naphthalene injection to ablate Clara cells (CC10$^+$) in these animals. Clara cells (*A*) were almost completely eliminated in this process (e.g., day 3 after naphthalene injection shown in *B*). Occasionally, cells that express both CGRP and CC10 can be found (arrow in *B*). Regeneration of surviving Clara cells was apparent by day 6 after naphthalene treatment (*D*). Naphthalene also induced PNEC proliferation as indicated by increased Ki67$^+$ PNECs (*F* and *G*). A time course of changes in the proliferation rate of PNECs after naphthalene treatment is shown in *H*. (*F Inset*) Individual images of CGRP and Ki67 immunostaining of the same cells. (*I–L*) Immunostaining of lung sections from adult $CGRP^{CreER/+}$;$ROSA26^{mTmG/+}$ mice 1 mo after naphthalene injection, which was performed following tamoxifen administration. The combined treatment of TM and naphthalene resulted in labeling of PNECs as well as Clara cells (CC10$^+$) and ciliated cells [acetylated (Ac)-tubulin$^+$] (*I–L*). No other cell types were labeled by eGFP, which is in contrast to the stable lineage of PNECs during homeostasis. Note that *L* is a merged image of *I–K*. (Scale bars: 25 μm for panels in each column.)

type II cells, were unaffected in $CGRP^{CreER/+}$;$ROSA26^{DTA/+}$ mice (Fig. S5). We collected lungs from $CGRP^{CreER/+}$;$ROSA26^{DTA/+}$ mice at 1, 6, 10, and 12 mo post-TM injection, and at no time points could we detect regenerated PNECs (Fig. 3 *A* and *B*). We conclude that once ablated PNECs cannot be replaced by other cell types during homeostasis.

We also tested whether PNECs, once eliminated, can be regenerated during lung injury in $CGRP^{CreER/+}$;$ROSA26^{DTA/+}$ mice. In this study, we ablated PNECs in $CGRP^{CreER/+}$;$ROSA26^{DTA/+}$ mice by TM injection and then induced lung injury with naphthalene, which can stimulate PNEC proliferation as described above. No PNEC regeneration was found 1 mo after naphthalene injection (Fig. 3*F*), by which time Clara cells had fully regenerated. Furthermore, even with repeated naphthalene-induced lung injury, we observed no evidence of PNEC recovery. Taken together, these results indicate the inability of other lung cells types to replenish PNECs during homeostasis or following tissue injury, turnover of PNECs seems to be the only mechanism of their renewal.

Selective Ablation of Pulmonary Neuroendocrine Cells Does Not Affect Clara Cell Regeneration Following Naphthalene-Induced Lung Injury. PNECs are found in close association with Clara cells, in particular, the naphthalene-resistant Clara cells, which led to the

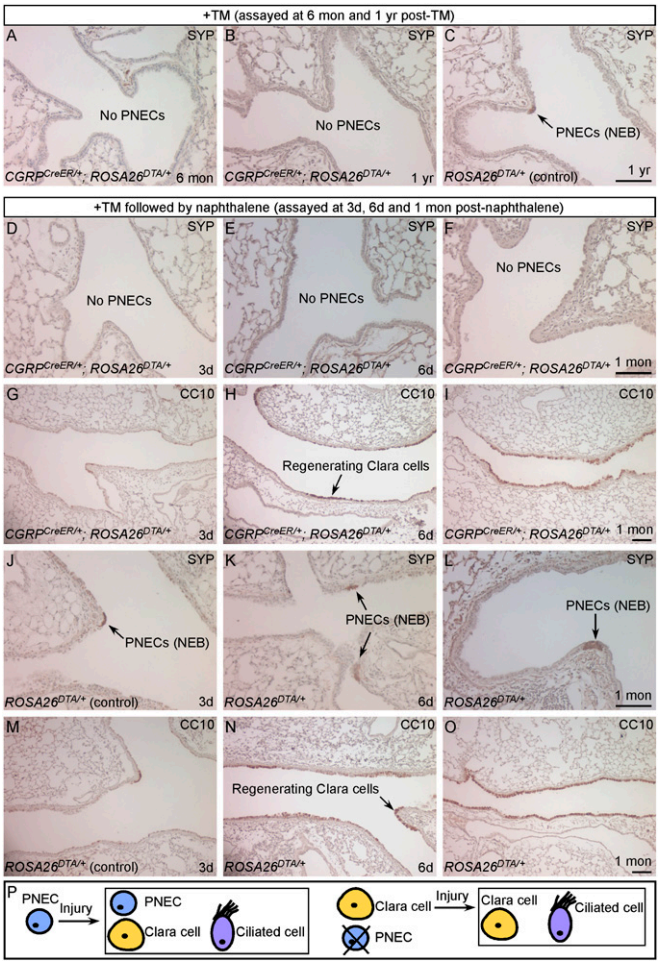

Fig. 3. PNECs are dispensable for Clara cell regeneration during naphthalene-induced lung injury. (*A*–*C*) Immunostaining of lung sections from adult *CGRP*$^{CreER/+}$;*ROSA26*$^{DTA/+}$ (experimental) and *ROSA26*$^{DTA/+}$ (control) mice. Activation of CreER by TM induced DTA expression in *CGRP*$^{CreER/+}$;*ROSA26*$^{DTA/+}$ adult lungs, resulting in efficient killing of PNECs. PNECs (SYP$^+$ or CGRP$^+$) or NEBs could not be detected in these animals (*A* and *B*), whereas other cell types were unaffected (Fig. S5). Long-term tracing of PNECs in adult *CGRP*$^{CreER/+}$;*ROSA26*$^{DTA/+}$ mice showed no sign of PNEC replenishment. (*D*–*I*) Immunostaining of lung sections from adult *CGRP*$^{CreER/+}$;*ROSA26*$^{DTA/+}$ mice. Activation of CreER by TM in adult lungs induced DTA expression, resulting in efficient PNEC ablation. These mice were subsequently treated with naphthalene to ablate Clara cells (CC10$^+$). Despite the absence of PNECs (*D*–*F*), Clara cell regeneration followed a time course (*G*–*I*) similar to that in control mice (*M*–*O*). Extensive Clara cell proliferation was observed by day 6 after naphthalene injection (*H*), and Clara cells had fully regenerated by 1 mo after the initial insult (*I*). (*J*–*O*) Immunostaining of lung sections from adult *ROSA26*$^{DTA/+}$ control mice that received an identical regimen of TM and naphthalene treatment. PNECs (arrows in *J*–*L*) were unaffected, and the distribution of lung cell types and the kinetics of Clara cell regeneration (*M*–*O*) are similar to those in WT mice. (*P*) A model of PNEC specification and function during lung injury. (Scale bars: 100 μm for panels in each row)

speculation that PNECs maintain a stem cell niche essential for Clara cell regeneration during lung injury. We used *CGRP*$^{CreER/+}$;*ROSA26*$^{DTA/+}$ mice in which PNECs have been ablated to test this hypothesis. We injected *CGRP*$^{CreER/+}$;*ROSA26*$^{DTA/+}$ mice with TM, followed by naphthalene administration. PNECs in *CGRP*$^{CreER/+}$;*ROSA26*$^{DTA/+}$ lungs were almost completely eliminated as revealed by immunostaining (Fig. 3 *D*–*F* and Fig. S5) compared with intact PNECs in *ROSA26*$^{DTA/+}$ controls (Fig. 3 *J*–*L*). At 3 d after naphthalene treatment, the majority of Clara cells were already killed and released from the airway basement membrane in both *CGRP*$^{CreER/+}$;*ROSA26*$^{DTA/+}$ (Fig. 3*G*) and *ROSA26*$^{DTA/+}$ (Fig. 3*M*) lungs. By day 6, nascent regenerating Clara cells comprised 40% of the total airway epithelium in PNEC-ablated (Fig. 3*H*) and control (Fig. 3*N*) lungs. After 1 mo, similar to *ROSA26*$^{DTA/+}$ lungs (Fig. 3*O*), Clara cells had almost completely regenerated in *CGRP*$^{CreER/+}$;*ROSA26*$^{DTA/+}$ lungs (Fig. 3*I*), whereas PNECs remained absent (Fig. 3*F*). To rule out the possibility that Clara cells in contact with PNECs before PNEC ablation had already received inductive signals and acquired the potential to regenerate, we repeated naphthalene-induced lung injury and still observed equally efficient Clara cell regeneration. In all of these studies, there was no difference in the kinetics of Clara cell regeneration between *CGRP*$^{CreER/+}$;*ROSA26*$^{DTA/+}$ and *ROSA26*$^{DTA/+}$ mice, which suggests that Clara cell regeneration can occur in the absence of PNECs. Previous studies suggest that a small population of CGRP$^+$;CC10$^+$ cells within NEBs may give rise to regenerated Clara and ciliated cells during naphthalene-induced lung injury. We found very few CGRP$^+$;CC10$^+$ cells in naphthalene-injured lungs (Fig. 2*B*) and did not detect these doubly positive cells in uninjured or PNEC-ablated lungs. This population is thus unlikely to account for the speedy and extensive Clara cell regeneration after naphthalene-induced lung injury and is also incapable of replenishing ablated PNECs.

Inactivation of *p53*, *Rb*, and *Pten* in Pulmonary Neuroendocrine Cells Leads to SCLC. Because up to 90% of human SCLCs have sustained mutations in the tumor suppressors *p53* and *Rb*, we used the *CGRP*^{CreER} mouse line to inactivate both *p53* and *Rb* in PNECs. We bred mice to produce *CGRP*$^{CreER/+}$;*p53*$^{f/f}$;*Rb*$^{f/f}$ mice (f: floxed) and delivered TM to these animals. We found that selective removal of *p53* and *Rb* in PNECs resulted in PNEC hyperplasia and tumor development a few months after TM administration (e.g., 5–6 mo post-TM; Fig. 4*B*). In our study, among 32 TM-injected *CGRP*$^{CreER/+}$;*p53*$^{f/f}$;*Rb*$^{f/f}$ adult mice at 5–6 mo of age, 4 developed PNEC hyperplasias and small lung tumors (Fig. 4*B*), 12 developed PNEC hyperplasia, and 16 had no obvious morphological defects. Because *Pten* mutations are also found in a significant number of human SCLCs (19, 20), we speculated that mutations in *Pten* could cooperate with *p53*/*Rb* mutations to promote SCLC development. Indeed, loss of *Pten*, in addition to *p53* and *Rb*, significantly accelerated tumor initiation and progression. Analysis of these triple-mutant mice at 2–4 wk after TM administration revealed the presence of small hyperplastic lesions that are likely the precursors for SCLC (Fig. 4*C*). Compared with *CGRP*$^{CreER/+}$;*p53*$^{f/f}$;*Rb*$^{f/f}$ mice at the same stage, not only more and larger PNEC hyperplasias and SCLC tumors were present in the sections of *CGRP*$^{CreER/+}$;*p53*$^{f/f}$;*Rb*$^{f/f}$; *Pten*$^{f/f}$ lungs (Fig. 4 *C* and *F*), but unlike double-mutant mice, these lesions in triple-mutant mice at 2.5 mo post-TM showed signs of tumor invasiveness. For instance, malignant tumor cells (Fig. 4*D*) can be found surrounding and inside blood vessels (Fig. 4*E*). A total of 17/17 TM-injected *CGRP*$^{CreER/+}$;*p53*$^{f/f}$;*Rb*$^{f/f}$;*Pten*$^{f/f}$ adult mice developed PNEC hyperplasias (Fig. 4*C*) and large lung tumors (Fig. 4*F*) at 2–3 mo of age. All double- and triple-mutant mice analyzed developed thyroid tumors (Fig. S6). Most double-mutant mice died within 6–7 mo, and triple-mutant mice died within 3 mo after TM injection, likely due to lesions in the lung and thyroid (Fig. S6). These results are consistent with a model in which loss of tumor suppressors leads to progressive acquisition of tumor properties.

Tumors developed in *p53*/*Rb* double-knockouts or *p53*/*Rb*/*Pten* triple-knockout mice are comprised of Ki67$^+$ proliferating cells (Fig. 4*G*) that express neuroendocrine markers (Fig. 4 *H* and *I*). The proliferation rate increased considerably with time (Fig. 4 *J*–*O*), and lesions in *p53*/*Rb*/*Pten* mice had a higher rate of proliferation than those in *p53*/*Rb* mice at any time point post-TM (Fig. 4*L*). In fact, significant PNEC proliferation was apparent even 1 wk post-TM in *p53*/*Rb*/*Pten* mice (Fig. 4*K*). These observations confirm and extend previous reports (12–15) suggesting that PNECs can be the cells of origin for SCLC, offering insight

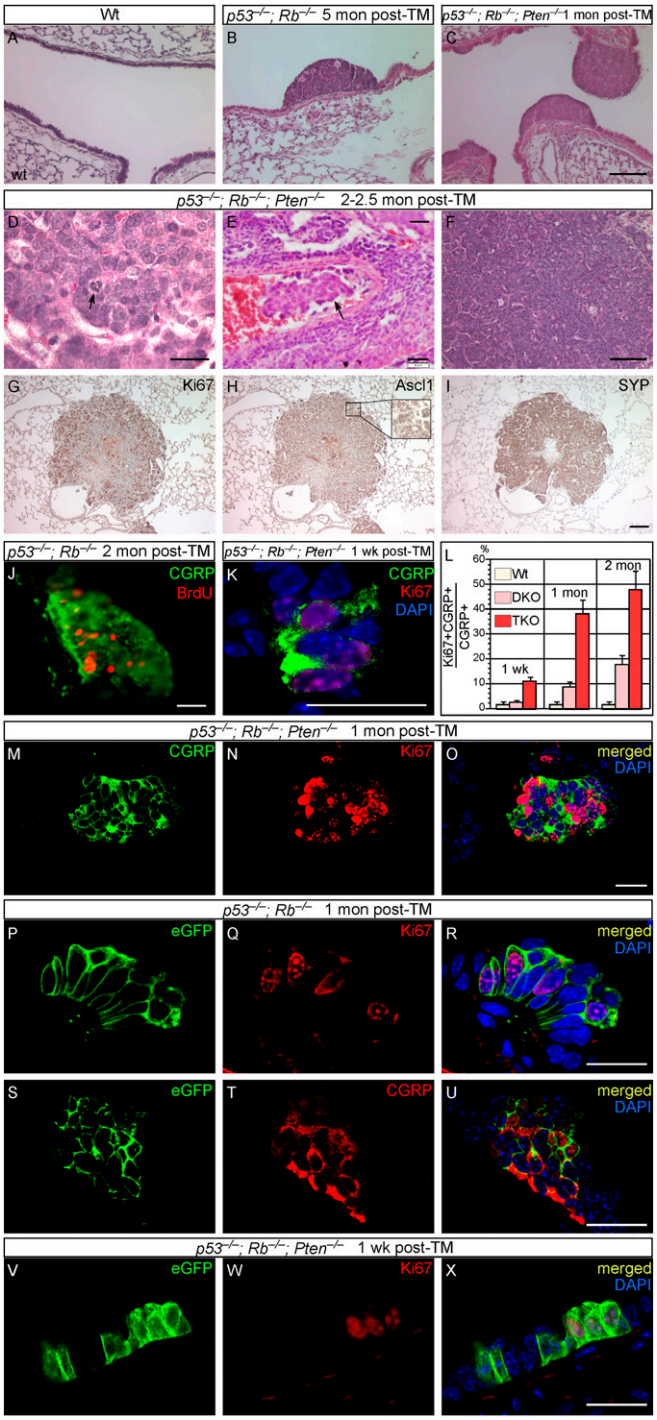

Fig. 4. SCLC can originate from differentiated PNECs. (*A–I*) Histology and immunostaining of lung sections from WT, $CGRP^{CreER/+};p53^{f/f};Rb^{f/f}$ [double knockout (DKO)], and $CGRP^{CreER/+};p53^{f/f};Rb^{f/f};Pten^{f/f}$ [triple knockout (TKO)] adult mice. Cancer cells in triple-mutant mice displayed aberrant mitosis (arrow in *D*) and also showed signs of tumor invasiveness (arrow in *E*). Tumors are comprised of proliferating Ki67$^+$ cells (*G*) and also expressed neuroendocrine markers such as Ascl1 (Mash1) (*H*) and SYP (*I*). (*J–O*) Immunostaining of lung sections from WT, $CGRP^{CreER/+};p53^{f/f};Rb^{f/f}$, and $CGRP^{CreER/+};p53^{f/f};Rb^{f/f};Pten^{f/f}$ adult mice. PNECs lacking *p53* and *Rb* displayed extensive PNEC proliferation as judged by Ki67 staining (*J*). Proliferating PNECs could be found 1 wk after TM injection (*K*) in triple-mutant mice, and the proliferation rate increased substantially with time (*L–O*). (*P–X*) Immunostaining of lung sections from WT, $CGRP^{CreER/+};ROSA26^{mTmG/+};p53^{f/f};Rb^{f/f}$, and $CGRP^{CreER/+};ROSA26^{mTmG/+};p53^{f/f};Rb^{f/f};Pten^{f/f}$ adult mice. TM injection selectively ablated *p53*/*Rb* or *p53*/*Rb*/*Pten* in PNECs, which were simultaneously labeled by eGFP. Inactivating *p53* and *Rb* in PNECs (CGRP$^+$) (*T*) led to extensive PNEC proliferation as observed by Ki67 staining (*Q*). Most, if not all PNECs, were also labeled by eGFP (*P* and *S*), suggesting that differentiated PNECs proliferated and subsequently led to tumor growth. Similarly, TM injection into $CGRP^{CreER/+};ROSA26^{mTmG/+};p53^{f/f};Rb^{f/f};Pten^{f/f}$ mice labeled proliferating PNECs (*V* and *W*), which likely led to tumor development. (Scale bars: *A–C* and *F–I*, 100 μm; *D*, *E*, *J*, *K*, and *M–X*, 20 μm.)

into the complex interactions between tumor suppressors in tumor development.

SCLC Can Originate from Differentiated Pulmonary Neuroendocrine Cells. Our $CGRP^{CreER/+}$ mice offer an opportunity to examine tumor initiation and progression by labeling PNECs and following their fate over time; this was achieved by producing $CGRP^{CreER/+};ROSA26^{mTmG/+};p53^{f/f};Rb^{f/f}$ mice. In differentiated PNECs where $CGRP^{CreER}$ is expressed and activated by TM to remove *p53* and *Rb*, these cells are also permanently labeled with eGFP (from $ROSA26^{mTmG}$; Fig. 4 *P* and *S*), allowing us to follow their fate during subsequent steps of cell transformation and tumor development. We examined labeled PNEC cells in $CGRP^{CreER/+};ROSA26^{mTmG/+};p53^{f/f};Rb^{f/f}$ lungs at various time points after TM injection. We found that almost all CGRP$^+$ cells within the early hyperplastic lesions (i.e., containing a couple of dozen cells; Fig. 4*T*) were also labeled by eGFP (Fig. 4 *P* and *S*), and many of the labeled PNECs were actively dividing (Fig. 4*Q*). Similarly, TM injection into $CGRP^{CreER/+};ROSA26^{mTmG/+};p53^{f/f};Rb^{f/f};Pten^{f/f}$ mice labeled proliferating PNECs, which likely led to tumor development (Fig. 4 *V–X*). Thus, the majority of, if not all, labeled proliferating PNECs in the hyperplasic lesions and tumors are derived from PNECs that express multiple differentiation markers. These results support the idea that SCLC can originate from differentiated PNECs within NEBs.

Discussion

Compared with other lung cell types, in vivo analysis of PNECs is underexplored. In this study, we report a genetic tool to investigate PNEC lineage and function. Our data suggest that PNECs may share a common lineage with alveolar cells either from common or separate progenitors during lung development but can contribute to Clara cells and ciliated cells in lung injury (Figs. 1 *P* and *Q* and 3*P*). The distinct cell fates adopted by PNECs during homeostasis and injury clearly demonstrate the plasticity of PNECs, and places PNECs in the same category as basal cells, Clara cells, and type II cells, which can contribute to other cell types under different conditions. Different types of insults to lung epithelium induce distinct tissue responses. For instance, bleomycin administration eliminates alveolar cells and causes fibrosis without apparent regeneration. By contrast, influenza viral infection also kills alveolar cells, but these cells are replenished through progenitor cell proliferation (21). It is possible that with other forms of injury not tested in this study, PNECs can be induced to give rise to additional cell types. Interestingly, PNECs cannot be replenished once ablated during homeostasis or naphthalene-induced lung injury. Similarly, a different type of lung injury may induce PNEC regeneration. In all of these settings, the signals that trigger cell proliferation and fate change remain to be further investigated (22). Our results are consistent with the model in which homeostasis and tissue injury provide distinct microenvironments for maintaining an intact epithelium, because each context directs PNECs to generate different cell types.

PNECs have been implicated in multiple aspects of lung functions, including airway oxygen sensing, regulation of pulmonary blood flow, control of bronchial tonus, modulation of immune responses, and maintenance of a stem cell niche. These diverse activities are likely mediated by the amines and peptides released from PNECs, but their in vivo relevance is largely unconfirmed. Our $CGRP^{CreER}$ mice offer a unique opportunity to test these hypotheses. Mice in which PNECs are ablated peri- or

GENETICS

postnatally provide an ideal setting to explore various physiological functions of PNECs.

Contrary to the current model, our results demonstrate that PNEC ablation has no apparent effect on Clara cell regeneration in naphthalene-induced lung injury. Though we cannot formally exclude the possibility that a very small number of residual PNECs maintain a stem cell niche required for Clara cell recovery, the speedy and extensive regeneration of Clara cells even after repeated injury renders such a possibility remote, which suggests that signals derived from cells other than PNECs are responsible for Clara cell proliferation. Nonetheless, PNECs may play a redundant role or be required for Clara cell regeneration in other forms of injury.

Mouse models of SCLC have been reported in which tumor suppressors *p53* and *Rb* are inactivated in the lung epithelium via intrabronchial injection of adenoviral Cre (12) or an adenovirus (Ade-CGRP-Cre) in which a ∼2-kb rat *CGRP* promoter was used to drive Cre expression (13). Ade-CGRP-Cre is expressed in PNECs as well as in a small number of Clara cells and ciliated cells (13). Importantly, these mouse models recapitulate critical aspects of human SCLC. Our CreER-based genetic system complements studies using an adenovirus-based approach. In particular, our genetic system allows us to manipulate gene activity and label PNECs to follow their progression during tumor development. We observed earlier lethality associated with severe defects in the lung and/or other neuroendocrine organs when using the murine CreER system activated by full doses of TM injection. Though earlier lethality may limit the study of tumor metastasis, it has no impact on investigations of tumor initiation and progression. Furthermore, we expect to overcome this problem by injecting a lower dose of TM or by transplantation of tumors into a host mouse to study tumor behavior over an extended time course. Our results suggest that major tumor suppressors display complex interactions in SCLC development. Though removal of *Pten* in the background of *p53*/*Rb* mutations accelerates tumor development and confers tumor invasiveness, loss of *p53* and *Pten* does not appear to exert obvious effects within the same time frame. Identifying genes and pathways perturbed in tumors at various stages of progression would be a critical step toward understanding how these tumor suppressors individually and in combination control tumor development.

Our investigation of the relationship between PNECs and SCLC offers insight into the early stages of SCLC development (Fig. S6). Labeled PNECs within NEBs proliferate in early hyperplastic lesions. These cells, characterized by expression of all known PNEC markers, constitute the majority of dividing cells within the hyperplastic lesions upon removal of tumor suppressors. Tumors most likely are derived from proliferating PNECs. These findings provide strong evidence to support the notion that SCLC can originate from terminally differentiated PNECs that seldom proliferate during homeostasis. We cannot rule out the possibility that a subpopulation of PNECs that expresses low levels of CGRP and possesses special properties can constitute the cell of origin of SCLC. However, a very high percentage of labeled PNECs at early stages of tumor development after removal of *p53*/*Rb* or *p53*/*Rb*/*Pten* would suggest that if such a PNEC subpopulation exists, it is either prevalent or highly proliferative for an extended period to generate tumors. In this scenario, in contrast to the high proliferative potential of this special PNEC subpopulation, the rest of differentiated PNECs lacking *p53*/*Rb* or *p53*/*Rb*/*Pten* can only undergo limited division and do not contribute significantly to tumor formation. Without additional markers, distinguishing distinct subpopulations of differentiated PNECs is not currently feasible. In this regard, our $CGRP^{CreER}$ system provides a means to isolate a pure population of PNECs through fluorescence-activated cell sorting for molecular characterization.

Though PNECs can give rise to SCLC, ablation of *p53* and *Rb* in surfactant associated protein C-positive ($SP\text{-}C^{+}$) cells using an adenoviral approach also leads to SCLC, albeit at a much lower rate (13). It is unclear how the loss of tumor suppressors in $SP\text{-}C^{+}$ cells allows these cells to acquire neuroendocrine properties. Whether other cell types can also give rise to SCLC has not been extensively examined. We surmise that during tumor development, cells are converted to relatively immature (or uncommitted) states that reflect their developmental origin. In this case, it is interesting to note that PNECs and alveolar cells may share a common lineage during lung development. Genomic studies would be instrumental in identifying genes and pathways that underlie early stages of transformation in PNECs or other lung cell types—some of them would be ideal candidates for early diagnosis of SCLC or driver mutations that can be tailored for targeted therapies.

Materials and Methods

Mouse strains and standard procedures used in this study are described in *SI Materials and Methods*.

ACKNOWLEDGMENTS. We thank Peter Baluk for discussion on cardiomyocytes in the pulmonary vein and Ming-Tseh Lin for advice on tumor histology.

1. Morrisey EE, Hogan BL (2010) Preparing for the first breath: Genetic and cellular mechanisms in lung development. *Dev Cell* 18(1):8–23.
2. Domyan ET, Sun X (2011) Patterning and plasticity in development of the respiratory lineage. *Dev Dyn* 240(3):477–485.
3. Warburton D, et al. (2010) Lung organogenesis. *Curr Top Dev Biol* 90:73–158.
4. Cardoso WV, Whitsett JA (2008) Resident cellular components of the lung: Developmental aspects. *Proc Am Thorac Soc* 5(7):767–771.
5. Linnoila RI (2006) Functional facets of the pulmonary neuroendocrine system. *Lab Invest* 86(5):425–444.
6. Domnik NJ, Cutz E (2011) Pulmonary neuroepithelial bodies as airway sensors: Putative role in the generation of dyspnea. *Curr Opin Pharmacol* 11(3):211–217.
7. Mahvi D, Bank H, Harley R (1977) Morphology of a naphthalene-induced bronchiolar lesion. *Am J Pathol* 86(3):558–572.
8. Stripp BR, Maxson K, Mera R, Singh G (1995) Plasticity of airway cell proliferation and gene expression after acute naphthalene injury. *Am J Physiol* 269(6 Pt 1): L791–L799.
9. Reynolds SD, Giangreco A, Power JH, Stripp BR (2000) Neuroepithelial bodies of pulmonary airways serve as a reservoir of progenitor cells capable of epithelial regeneration. *Am J Pathol* 156(1):269–278.
10. Reynolds SD, et al. (2000) Conditional Clara cell ablation reveals a self-renewing progenitor function of pulmonary neuroendocrine cells. *Am J Physiol Lung Cell Mol Physiol* 278(6):L1256–L1263.
11. van Meerbeeck JP, Fennell DA, De Ruysscher DK (2011) Small-cell lung cancer. *Lancet* 378(9804):1741–1755.
12. Meuwissen R, et al. (2003) Induction of small cell lung cancer by somatic inactivation of both Trp53 and Rb1 in a conditional mouse model. *Cancer Cell* 4(3):181–189.
13. Sutherland KD, et al. (2011) Cell of origin of small cell lung cancer: Inactivation of Trp53 and Rb1 in distinct cell types of adult mouse lung. *Cancer Cell* 19(6): 754–764.
14. Park KS, et al. (2011) Characterization of the cell of origin for small cell lung cancer. *Cell Cycle* 10(16):2806–2815.
15. Schaffer BE, et al. (2010) Loss of p130 accelerates tumor development in a mouse model for human small-cell lung carcinoma. *Cancer Res* 70(10):3877–3883.
16. Rawlins EL, Clark CP, Xue Y, Hogan BL (2009) The Id2+ distal tip lung epithelium contains individual multipotent embryonic progenitor cells. *Development* 136(22): 3741–3745.
17. Mueller-Hoecker J, et al. (2008) Of rodents and humans: A light microscopic and ultrastructural study on cardiomyocytes in pulmonary veins. *Int J Med Sci* 5(3):152–158.
18. Rawlins EL, et al. (2009) The role of Scgb1a1+ Clara cells in the long-term maintenance and repair of lung airway, but not alveolar, epithelium. *Cell Stem Cell* 4(6):525–534.
19. Yokomizo A, et al. (1998) PTEN/MMAC1 mutations identified in small cell, but not in non-small cell lung cancers. *Oncogene* 17(4):475–479.
20. Kim SK, et al. (1998) Alterations of PTEN/MMAC1, a candidate tumor suppressor gene, and its homologue, PTH2, in small cell lung cancer cell lines. *Oncogene* 16(1):89–93.
21. Kumar PA, et al. (2011) Distal airway stem cells yield alveoli in vitro and during lung regeneration following H1N1 influenza infection. *Cell* 147(3):525–538.
22. Xing Y, Li A, Borok Z, Li C, Minoo P (2012) NOTCH1 is required for regeneration of Clara cells during repair of airway injury. *Stem Cells* 30(5):946–955.